

**Fermi National Accelerator Laboratory**

**FERMILAB-FN-624**

# **The Effects of Miscalibration on the Energy Resolution of the CMS Calorimeter**

**A. Beretvas et. al**

*Fermi National Accelerator Laboratory  
P.O. Box 500, Batavia, Illinois 60510*

**August 1994**

## **Disclaimer**

*This report was prepared as an account of work sponsored by an agency of the United States Government. Neither the United States Government nor any agency thereof, nor any of their employees, makes any warranty, express or implied, or assumes any legal liability or responsibility for the accuracy, completeness, or usefulness of any information, apparatus, product, or process disclosed, or represents that its use would not infringe privately owned rights. Reference herein to any specific commercial product, process, or service by trade name, trademark, manufacturer, or otherwise, does not necessarily constitute or imply its endorsement, recommendation, or favoring by the United States Government or any agency thereof. The views and opinions of authors expressed herein do not necessarily state or reflect those of the United States Government or any agency thereof.*

# **The Effects of Miscalibration on the Energy Resolution**

A. Beretvas, J. Freeman, D. Green, J. Marraffino, and W. Wu

Fermi National Accelerator Laboratory, Batavia, Illinois, 60510.

Version 1.0 August 12, 1994.

## **1 Introduction**

We have studied the degradation in the performance of the CMS hadron calorimeter due to different types of miscalibrations. The CMS hadron calorimeter will have copper as its absorber and will be located in a high magnetic field (4 Tesla). The active element consists of plastic scintillator plates read out with WaveLength Shifting (WLS) fibers. The miscalibrations studied here are of two types, random tile-to-tile variations, and systematic front-to-back variations. We have developed algorithms to compensate for the miscalibrations, using hadron data from the LAB E experiment. The energy resolution of the hadron calorimeter is defined to be of the form  $dE/E = a/\sqrt{E} \oplus b$ . The miscalibrations result in a larger constant term (b). These estimates of the constant term increase are used in turn to specify the required manufacturing tolerances.

## **2 CMS Hadron Calorimeter**

The CMS hadron calorimeter will have a tower granularity of about  $0.1 \times 0.1$  in  $\eta$ - $\phi$  space. The design has not yet been completed. However, it is expected that the towers in the central region

will contain about 18 active layers. The layers are grouped into 3 longitudinal regions (HAC1, HAC2, and “tail catcher”).

### 3 Experimental Hadron Data

We use hadron data from the LAB E experiment<sup>[1]</sup> to simulate the CMS hadron calorimeter. That hadron calorimeter was  $19.2 \lambda$  deep and was read out at sampling intervals of  $0.7 \lambda$  starting at  $0.3 \lambda$ . To simulate the CMS hadron calorimeter we consider the first 9 layers as being the copper absorber and active layers, the next two layers are the coil (and are turned off) and the next three layers are the “tail catcher”<sup>[2]</sup>. The energy deposited by the  $i$ ’th particle in layer  $l$  is called  $L_{il}$ . The total energy deposited in our simulation of the CMS calorimeter is obtained by summing over the 3 longitudinal regions ( $k = 1$  to 3):

$$E_i = \sum_{k=1}^3 \sum_{l=lmin(k)}^{lmax(k)} L_{il} \quad (1)$$

Note that test beam data with a steel calorimeter is used. The CMS coil is aluminum, so that the present analysis overestimates the effect of the inert coil material. The data set used here consists of pions incident at momentum of 25, 50, 200 and 450 GeV/c. The longitudinal shower profiles are illustrated in Figure 1.

### 4 Miscalibrations: Tile-to Tile variations

We first consider random tile-to-tile light yield variation. This variation occurs because of the effect of variation in tile thickness, variation of the WLS fiber length, nonuniformity of the mirrors at the ends of the WLS fibers, nonuniformity of the green-to-clear splices, variations in the length of the

clear fibers, variation in the transmission of the light across connectors and the coupling of the fibers to the readout photomultipliers. All such factors affects the variance of the tile/fiber assemblies. Stricter quality control implies increasing the cost, while on the other hand, looser criteria on tile-to-tile uniformity can degrade the calorimeter performance. In our study, we consider (case A) a 10% Gaussian fluctuation about the mean of the tile-to-tile response. We write this fluctuation for the  $j$ 'th tower in the  $l$ 'th layer as  $c_{jl}$ . Then the energy deposited by the  $i$ 'th particle in the  $j$ 'th tower is:

$$E_{ij} = \sum_{k=1}^3 \sum_{l=lmin(k)}^{lmax(k)} L_{il} c_{jl} \quad (2)$$

To obtain good statistics we have looped over each tower 100 times.

## 5 Miscalibrations: Front-to-Back light yield variations

Due to the projective geometry of the CMS detector, the tiles forming the inner layers of the calorimeter will be smaller than those of the outer layers. Radiation damage may be another source of front-to-back variation. This front to back variation results in a continuous change in response (slope variation). We will consider two cases; (B) a continuous slope response of 25% over the entire hadron calorimeter and (C) a continuous slope response of 25% over the regions HAC1, HAC2 and the tail-catcher with separate calibration of the HAC compartments. In both these cases we also include the 10% Gaussian fluctuation of case(A). In Table 1 we show the results for an ideal calorimeter that contains all the energy of the shower in both the longitudinal and transverse directions, the CMS calorimeter [3], and also the results for a realistic CMS calorimeter that includes variations in actual construction. For case (A) (tile-to-tile variation of 10%) we find

the calorimeter resolution is degraded by 5.6, 10.5, 24.3 and 36.1% for hadron beam energies of 25, 50, 200 and 450 GeV. For the worst case (C) the resolution is degraded by 6.5, 12.4, 29.7 and 44.8%.

## 6 Corrections using Longitudinal Profiles

The longitudinal tile-to-tile variation inside a tower can be taken out if one knows the average longitudinal profile of hadron showers and actual tile-to-tile variation (as can be measured by radioactive sources). The longitudinal profile can be taken from HFC<sup>[4]</sup>-like measurements or GEANT. By measuring the longitudinal development of the shower in a given tower(j) and depth(l) over many events, one can attempt to divide out the factor  $c_{jl}$  and obtain an energy resolution equivalent to the original CMS resolution. We will determine only a correction factor for each depth(k) and tower(j). The depth segmentation correction factor is:

$$R_{kj} = \frac{\sum_i \sum_{l=l_{\min}(k)}^{l_{\max}(k)} L_{il}}{\sum_i \sum_{l=l_{\min}(k)}^{l_{\max}(k)} c_{jl} L_{il}} \quad (3)$$

The corrected energy for the i'th particle in the j'th tower is then:

$$E'_{ij} = \sum_{k=1}^3 R_{kj} \sum_{l=l_{\min}(k)}^{l_{\max}(k)} c_{jl} L_{il} \quad (4)$$

Note that event by event fluctuations are not taken into account in this algorithm, but the mean shift (see Fig. 1) is corrected.

## 7 Radioactive Source Calibration

The above profile corrections are usually implemented using radioactive sources. These sources can be maintained with an accuracy of 2%. If we let  $m_{jl}$  be the measured tile-to-tile variation in tower(j) and layer (l), then equation 4 for the corrected energy  $E'_{ij}$  is obtained by replacing  $c_{jl}$  by  $m_{jl}$  in equation 3. The energy resolution for the degradation caused by using sources, with 2% RMS measurement error is given in Table 1. This case corresponds to that which would be obtained if the precalibration before data taking was done only using sources and not a test beam.

## 8 Weighting Strategy

We have done a study to optimize the CMS hadron calorimeter energy resolution by assigning constant weights to layers<sup>[3]</sup>. The fit yields a weight of 1.5 for the HAC2 layer upstream of the coil, and a weight of 2.0 for the three layers after the coil. The results for a realistic CMS calorimeter with the above weighting, using the profile corrections are given in Table 2.

Figure 2 shows the reconstructed energy for four different calorimeters. The first corresponds to the realistic CMS calorimeter with limited (degraded) depth. This includes both a 10% variation in tile-to-tile response and a 25% variation in slope over the 3 depth layers (HAC1,HAC2,“tail-catcher”) of the calorimeter. The second case corresponds to applying our constant weighting strategy to improve the response of the calorimeter, and applying a correction based on the longitudinal profile. The profile is assumed to be determined by sources that measure to a precision of 2%. Note that, although the low end leakage tail is reduced, some high side evens are induced by this procedure.

The optimized energy resolution using active weighting determines 3 weight factors  $W_k$ . This

weighting depends on the energy ratio of HAC1 to HAC2, and is illustrated as case 3 in figure 2.

The energy for particle (i) in tower j is:

$$E_{ij}^{\text{active}} = \sum_{k=1}^3 W_k R_{kj} \sum_{l=\text{lmin}(K)}^{\text{lmax}(k)} c_{jl} L_{il} \quad (5)$$

We see that the high-side tail is eliminated and the low side tail is reduced. The fourth case corresponds to an ideal calorimeter with infinite length ( $19.2\lambda$ ).

## 9 Stochastic and constant term

The single particle resolution has been parameterized as a stochastic term (a) and a constant term (b):

$$\frac{\Delta E}{E} = \frac{a}{\sqrt{E}} \oplus b \quad (6)$$

The symbol  $\oplus$  means the two terms are added in quadrature. The values of (a) and (b) are given in Table 3 and 4. The results for configuration C are given in Figure 3. As expected the stochastic term remains approximately constant (range is from 0.93 to 0.84). However, there is a large change in the constant term as we go from one configuration to another (This range is from 8.9% to 3.8%). We expect the constant term to be approximately 5.7% for the CMS configuration after we have applied a profile correction using sources and also have applied different weights to the layers in front and downstream of the coil.

## 10 Summary

We have seen that an ideal detector resolution ( $A = 0.838$ ,  $B = 0.038$ ) is seriously degraded as effects of finite depth, the solenoid in the middle of the calorimeter; and manufacturing tolerances



are considered ( $A = 0.929$ ,  $B = 0.089$ ). This degradation can largely be eliminated if we: measure the “as built” tile-to-tile variations, and make average corrections; and use weighting schemes to compensate for the finite depth of CMS and the presence of the solenoid inside the calorimeter ( $A = 0.874$ ,  $B = 0.051$ ).

## References

- [1] W. K. Sakumoto *et al.*, “Calibration of the CCFR Target Calorimeter” Nucl. Instr. and Meth. **A294**, 179 (1990). We have used the Lab E data, private communications from W. K. Sakumoto.
- [2] The resolution of the CMS hadron calorimeter will be better than our simulation because of the larger number of active layers (most likely 18 versus 14). A similar study for the SDC detector used simulated data with finer longitudinal segmentation. This study however had no data above 250 GeV. P. de Barbaro, A. Bodek and B. Winer, “The effects of Tile Miscalibrations on the Performance of the Tile/fiber Based Hadron Calorimeters”, U. of Rochester UR-1301(1993).
- [3] A. Beretvas, D. Green, J. Marraffino and W. Wu, “How to optimize the CMS Hadron Calorimeter by assigning weights to Layers”, Fermilab FN-619, May 1994.
- [4] A. Beretvas *et al.* “Beam Tests of composite calorimeter configurations from reconfigurable-stack calorimeter”, Nucl. Instr. and Meth. **A329**, 50 (1993).

C1	Infinite calorimeter $19.2 \lambda$				
C2	CMS $9.4 \lambda$ calorimeter and inert coil				
C3	same as C2 but degraded due to construction				
A	10% Gaussian Fluctuation tile-to-tile				
B	25% Slope response over the entire calorimeter				
C	25% Slope response over each longitudinal region				
Energy(GeV)	C1	C2	C3		
			A	B	C
25	16.87	18.63	19.67	19.75	19.85
Profile Corrected			18.36	18.44	18.41
Source Calibration			18.38	18.45	18.41
50	12.24	14.44	15.96	16.07	16.23
Profile Corrected			14.55	14.74	14.68
Source Calibration			14.55	14.75	14.76
200	6.11	7.53	9.36	9.53	9.77
Profile Corrected			7.50	7.60	7.68
Source Calibration			7.50	7.60	7.69
450	4.13	5.56	7.57	7.75	8.05
Profile Corrected			5.51	5.75	5.67
Source Calibration			5.51	5.75	5.73

Table 1: Fractional energy resolution in % for the hadron calorimeter

C1	Infinite calorimeter $19.2 \lambda$				
C2	CMS improved by weighting				
C3	same as C2 but degraded due to construction				
A	10% Gaussian Fluctuation tile-to-tile				
B	25% Slope response over the entire calorimeter				
C	25% Slope response over each longitudinal region				
Energy(GeV)	C1	C2	C3		
			A	B	C
25	16.87	17.87			
Source Calibration			17.46	17.78	17.51
50	12.24	13.45			
Source Calibration			13.64	13.81	13.84
200	6.11	7.11			
Source Calibration			7.20	7.33	7.36
450	4.13	5.13			
Source Calibration			5.13	5.32	5.40

Table 2: Fractional energy resolution in % for the hadron calorimeter

C1	Infinite calorimeter 19.2 $\lambda$		
C2	CMS 9.4 $\lambda$ calorimeter and inert coil		
C3	same as C2 but degraded due to construction		
A	10% Gaussian Fluctuation tile-to-tile		
B	25% Slope response over the entire calorimeter		
C	25% Slope response over each longitudinal region		
Stochastic (a)	0.838	0.884	
Constant (b)	0.038	0.058	
	A	B	C
Stochastic (a)	0.929	0.932	0.929
Constant (b)	0.086	0.086	0.089
Profile Corrected			
Stochastic (a)	0.858	0.883	0.884
Constant (b)	0.061	0.068	0.066
Source Calibration			
Stochastic (a)	0.859	0.884	0.876
Constant (b)	0.062	0.069	0.067

Table 3: Stochastic (a) and constant (b) terms for the hadron calorimeter resolution

C1	Infinite calorimeter $19.2 \lambda$				
C2	CMS improved by weighting				
C3	same as C2 but degraded due to construction				
A	10% Gaussian Fluctuation tile-to-tile				
B	25% Slope response over the entire calorimeter				
C	25% Slope response over each longitudinal region				
	C1	C2	C3		
Stochastic (a)	0.838	0.883			
Constant (b)	0.038	0.046			
Source Calibration			A	B	C
Stochastic (a)			0.874	0.883	0.891
Constant (b)			0.051	0.050	0.057

Table 4: Stochastic (a) and constant terms (b) for the hadron calorimeter resolution

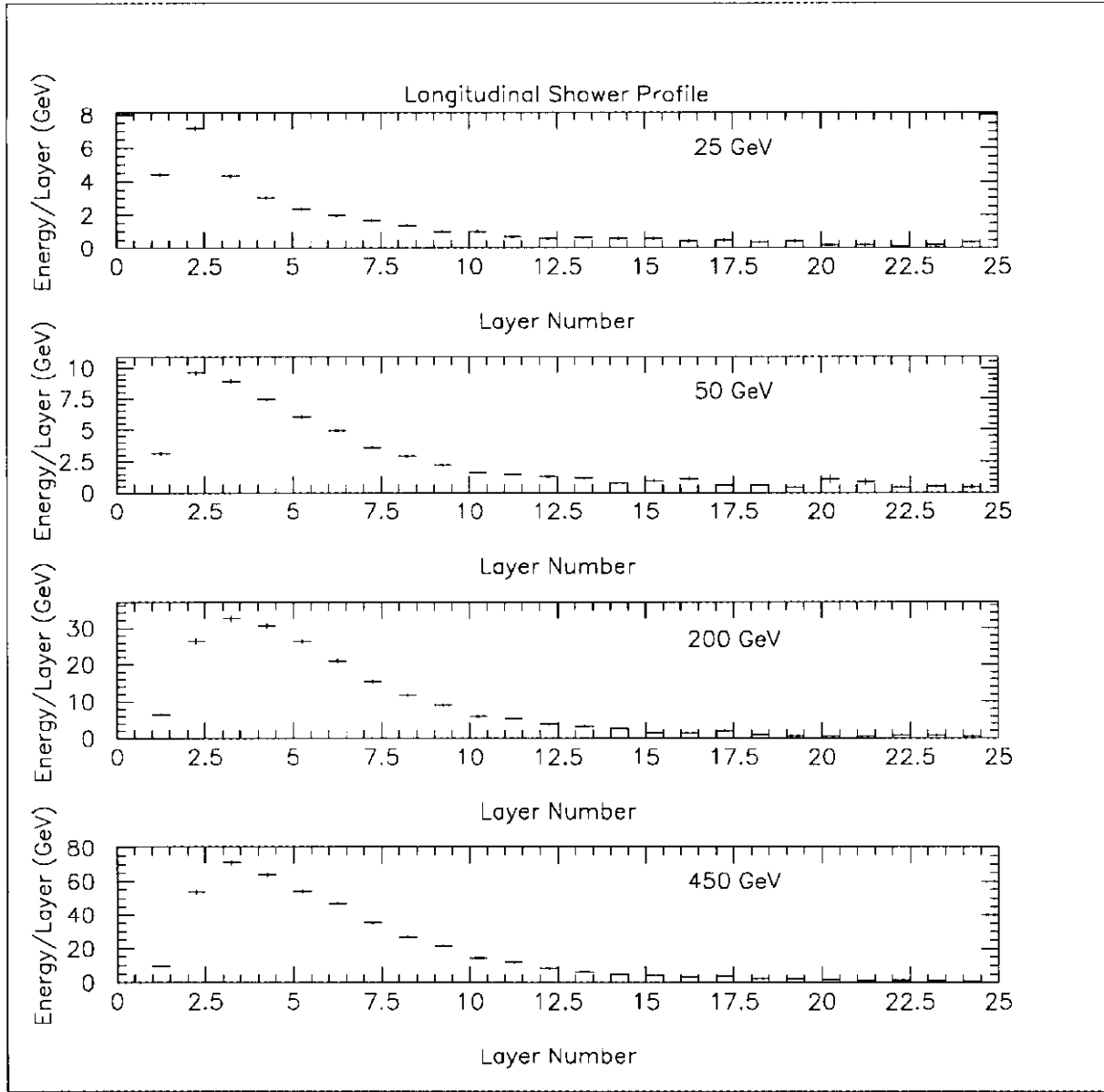


Figure 1: Longitudinal energy depth shower profile in a layer number for pion beams of energy 25, 50, 200 and 450 GeV. The vertical scale shows the energy(GeV) deposited in each layer.

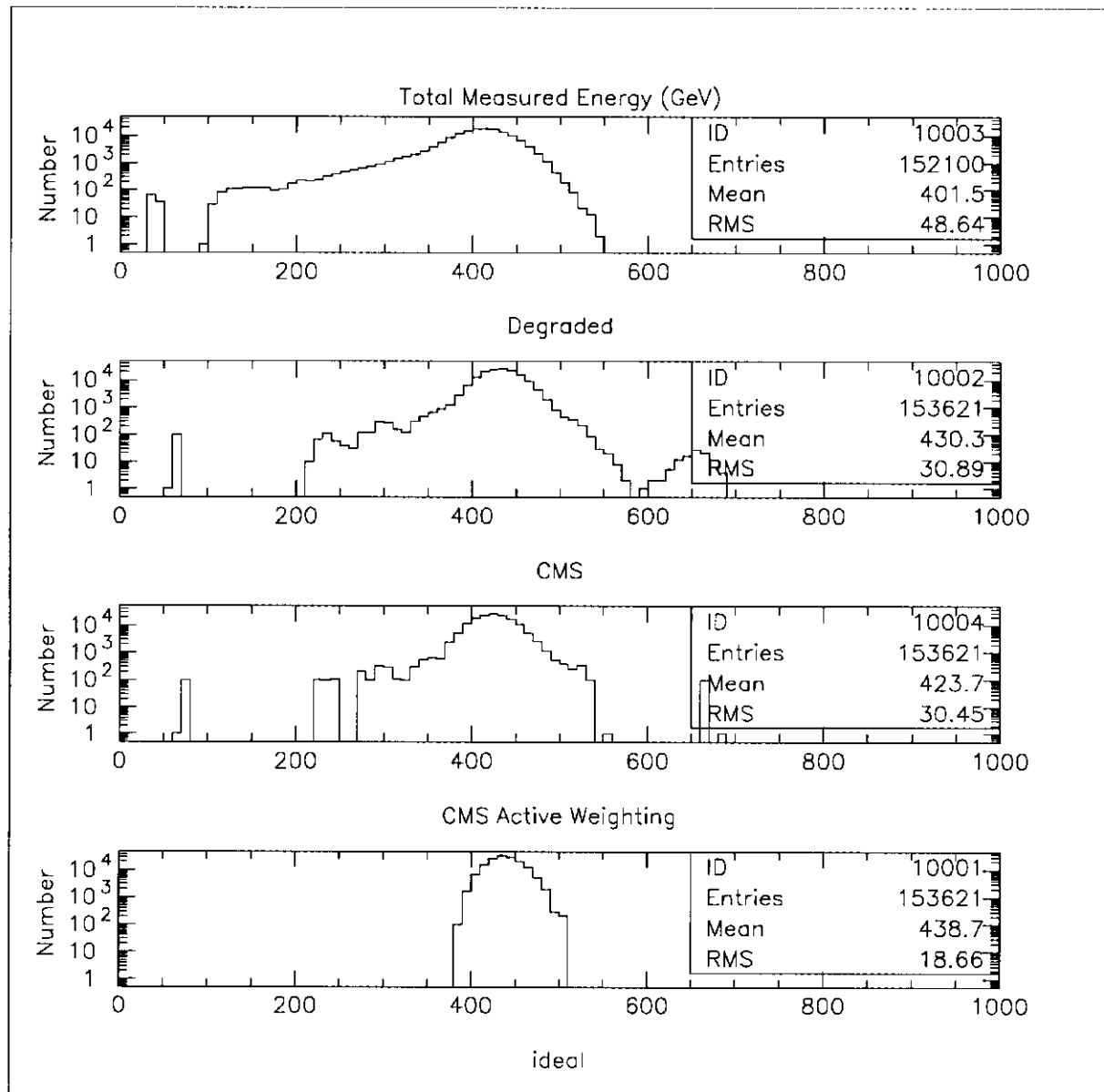


Figure 2: Reconstructed energy for 3 cases at 450 GeV. a) Degraded CMS calorimeter, b) Degraded calorimeter improved by both constant weighting and by using profile corrections maintained by a radioactive source c) Same as b) but using active weighting which depends on the ratio of energy in HAC1 to HAC2 d) ideal calorimeter



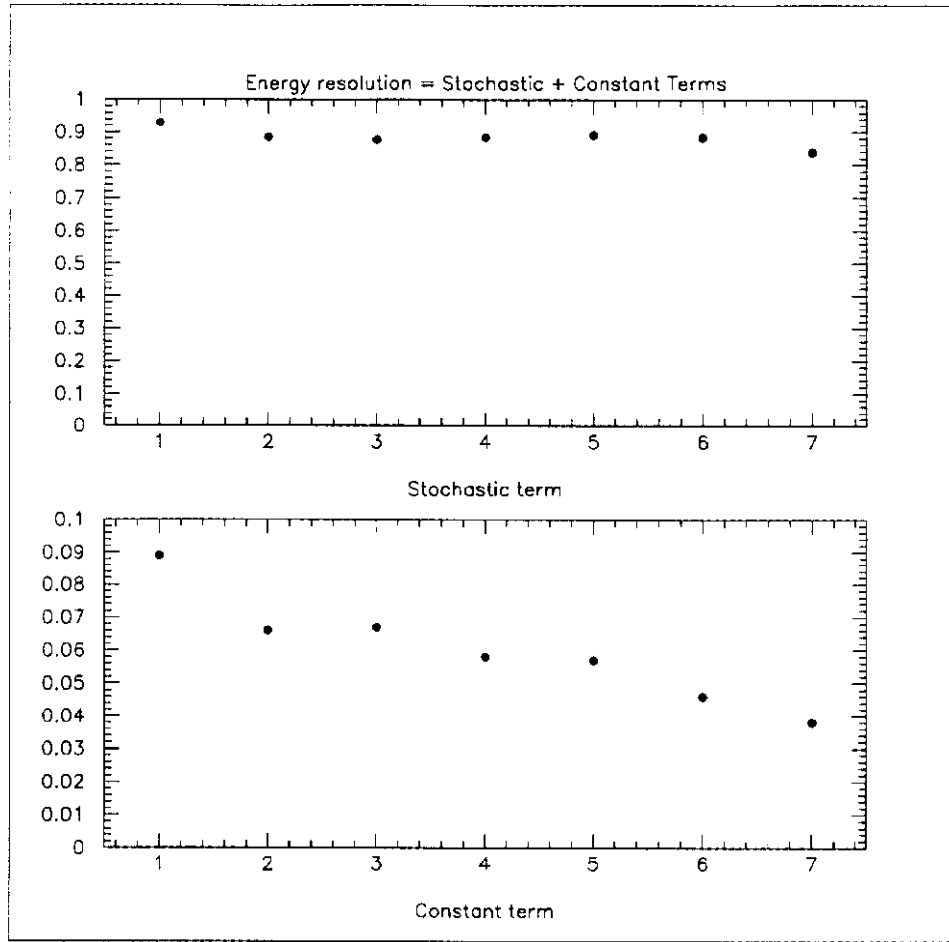


Figure 3: a) Stochastic parameter b) Constant parameter. Energy resolution for 7 different calorimeters

- 1) Degraded CMS (corresponding to a 10% tile=tile variation and a 25% slope variation for each depth
- 2) Same 1) only improved by using profile distribution
- 3) Same as 2) But monitored by a radioactive source to a precision of 2%
- 4) Standard CMS calorimeter
- 5) Realistic CMS calorimeter, corrected for profile and radioactive source, but also using constant weighting.
- 6) Standard CMS calorimeter with constant weighting.
- 7) Ideal (19.2 $\lambda$ ) Calorimeter